

\bar{p} - p Elastic and Charge Exchange Scattering at About 120 Mev

L. AGNEW, T. ELIOFF, W. B. FOWLER, L. GILLY, R. LANDER,
L. OSWALD, W. POWELL, E. SEGRÉ, H. STEINER, H. WHITE,
C. WIEGAND, AND T. YPSILANTIS

Radiation Laboratory, University of California, Berkeley, California
(Received March 31, 1958)

OBSERVATION of antiprotons in a propane or hydrogen bubble chamber offers the possibility of studying several phenomena which are less suitable to counter or photographic emulsion techniques.

The high ratio of pions, muons, and electrons to antiprotons in the available momentum-analyzed beams prevents the use of the bubble chamber without an initial purification, which increases the ratio of antiprotons to other particles in the beam. Such a purification has been achieved by utilizing the differential rate of momentum loss in absorbers between antiprotons and other particles. The principle of the method is to pass a momentum-analyzed beam through an absorber. Since particles of unequal mass will not have the same specific ionization, they will lose different amounts of momentum and a further magnetic deflection suffices to separate the particles physically according to mass. In this experiment, a desirable momentum for antiprotons entering the bubble chamber

was 684 Mev/ c ; however, at this momentum the ratio of undesirable particles to antiprotons at the target where they are produced is about 6×10^5 . By starting with 970-Mev/ c particles at the target and using the method of differential absorption, the ratio of undesirable particles (87% μ^- , 10% π^- , 3% e^-) to antiprotons entering the bubble chamber at 684 Mev/ c was decreased to 1.5×10^4 . A system of counters indicated when an antiproton entered the bubble chamber and although the chamber was expanded every bevatron pulse, the lights were flashed and the chamber photographed only when an antiproton entered.

The chamber has dimensions of 30 inches along the beam direction, 20 inches transverse to the beam, and 6.5 inches deep. It was filled with liquid propane of density 0.42 g cm^3 . Antiprotons entering the chamber with a momentum of 684 Mev/ c had an average range of 21 inches in propane; however, approximately 40% of the antiprotons never came to rest but rather annihilated in flight.

We have observed 478 antiprotons entering the chamber. One such event is shown in Fig. 1. The complete analysis of these events is in progress; however, a preliminary report on the \bar{p} - p elastic scattering is now available. A total of 33 \bar{p} - p elastic collisions have been observed over a path length of 179 meters.¹ The scatterings occur between 30 and 215 Mev with an average energy of 120 Mev. Only \bar{p} - p scatterings with angles $\geq 7.5^\circ$ (lab) were identifiable because otherwise the energy of the recoil proton was too small to make a visible track, so that these scatterings are indistinguishable from \bar{p} -C. A histogram showing the angular distribution of the scattering is given in Fig. 2 and has as a comparison a curve showing the result of a calculation by Fulco² based on the Ball-Chew³ model. The angular distributions are similar with an important preponderance of forward scattering, which is reasonably interpreted as the diffraction scattering connected with the annihilation. These angular distri-

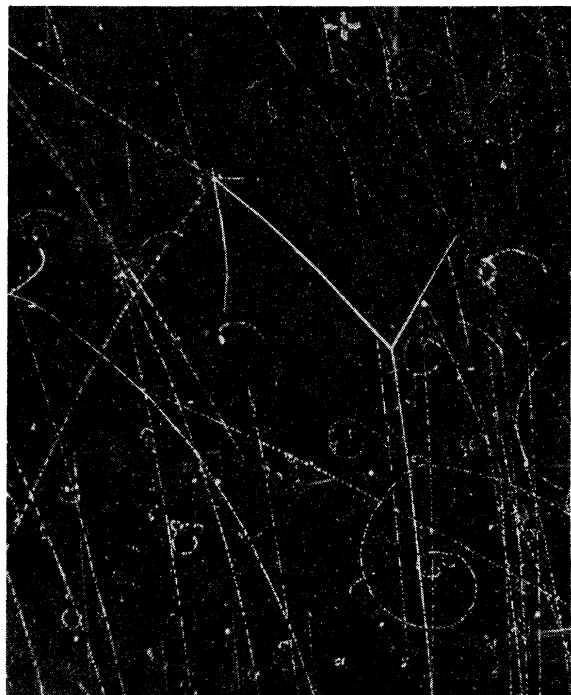


FIG. 1. \bar{p} - p scattering. The antiproton (denser track) enters from the top to the left of center. At an energy of 117 Mev, the antiproton scatters 41° to its left from a proton. The recoil proton has a range of 4.4 cm (49 Mev). The scattered antiproton comes to rest in 8.3 cm (68 Mev) and annihilates on a carbon nucleus, showing 5 visible prongs.

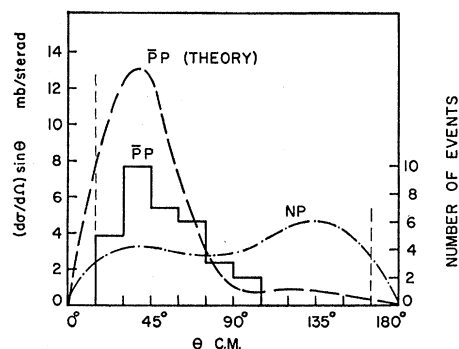


FIG. 2. \bar{p} - p elastic scattering at 120 Mev. The histogram shows the angular distribution of 33 observed \bar{p} - p scattering events between 15° and 165° center of mass. The dashed curve is the angular distribution calculated by Fulco. The n - p angular distribution is also shown for about the same energy [W. N. Hess, University of California Radiation Laboratory Report UCRL-4639 (unpublished)].

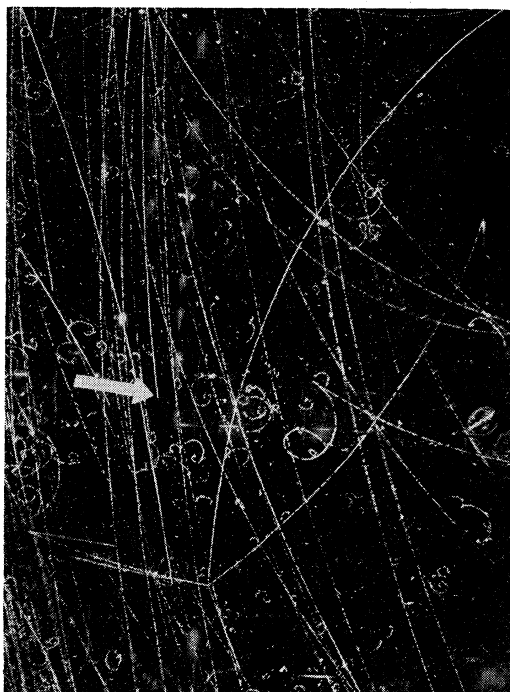


FIG. 3. An antiproton charge exchange. The antiproton is incident from the top and to the left of center, and the antiproton ending is indicated by an arrow. The antineutron from the charge-exchange process annihilates in the lower center of the picture. Five pions are produced in the annihilation with an energy release >1500 Mev.

butions differ markedly from the n - p which is also plotted for comparison. The total \bar{p} - p elastic cross section for scattering between 15° and 165° (center of mass) is 41_{-7}^{+10} mb. This should be compared to Fulco's value of 68 mb for the same angular interval.

The charge-exchange process $\bar{p} + p \rightarrow \bar{n} + n$ can be observed in the bubble chamber. One event has been identified and it is shown in Fig. 3 because of its inherent interest. The angle between the antiproton direction and the line connecting the antiproton ending with the vertex of the star is 30° in the lab system. The visible energy release in the star is >1500 Mev with the tentative identification of the annihilation products as $3\pi^+$ and $2\pi^-$. Thus the star is consistent with the process $\bar{n} + p \rightarrow 3\pi^+ + 2\pi^-$. The energy of the antiproton at the point of disappearance is estimated as 50 ± 30 Mev.

Other results such as the carbon annihilation and scattering cross sections and details of the annihilation process must await completion of the analysis.

¹ Five additional \bar{p} - p scattering events have been observed in nuclear emulsions by Chamberlain, Goldhaber, Jauneau, Kalogeropoulos, Segrè, and Silberberg. These are reported in the *Proceedings of the Padua-Venice Conference on Fundamental Particles, 1957* (Suppl. Nuovo cimento, to be published).

² Jose Fulco, Phys. Rev. **110**, 784 (1958) and University of California Radiation Laboratory Report UCRL-8183 (unpublished).

³ J. S. Ball and G. F. Chew, Phys. Rev. **109**, 1385 (1958).

9.51-Mev Level in N^{14}

D. M. ZIPOY

Laboratory of Nuclear Studies, Cornell University, Ithaca, New York

(Received March 10, 1958)

IT was pointed out recently¹ that the radiative decay angular distributions from the 9.51-Mev state in N^{14} were inconsistent with the spin assignment of $J=3$ reported in a paper on a $C^{13}(p,p)C^{13}$ experiment done previously,² but were consistent with a $J=2$ assignment. Because of this discrepancy, the analysis of the elastic scattering data was redone with the result that the assignment of $J^\pi=2^-$ does give a better fit than $J^\pi=3^-$. The resonance is fit well with a mixture of forty percent $S=1$ and sixty percent $S=0$ states and a level width of 40 kev. It is interesting to note that this mixture corresponds to $j=\frac{5}{2}$ with essentially no contribution from $j=\frac{3}{2}$, where j is the sum of the orbital angular momentum and one of the spins; j is then combined with the other spin to give J . An assignment of $J^\pi=1^-$ for the level gives a very poor fit, as do any other assignments with the possible exception of $J^\pi=3^-$ mentioned previously.

Because of the interference between the 9.39- and 9.51-Mev levels, the width of the 9.39-Mev level changed to about 20 kev; the assignment is still 1^- .

¹ E. Warburton (private communication).

² Zipoy, Freier, and Famularo, Phys. Rev. **106**, 93 (1957).

Hyperfine Structure of Deuterium and Nucleon-Nucleon Spin-Orbit Potentials*

A. M. SESSLER, *The Ohio State University, Columbus, Ohio*

AND

H. M. FOLEY, *Columbia University, New York, New York*

(Received March 24, 1958)

THE original suggestion¹ that nucleon-nucleon forces include a spin-orbit term has recently been reconsidered by a number of authors.² The inclusion of such forces leads to a modification of the magnetic properties of the deuteron³ and in particular modifies the magnetic moment, as has been emphasized in a recent paper by Feshbach.⁴ It is the purpose of this note to point out that the hyperfine structure (hfs) of deuterium is a very sensitive indicator of the amount of spin-orbit forces in the deuteron; and that even with the present theoretical uncertainty in the interpretation of the hfs, it affords a limitation on the amount of magnetic moment arising from spin-orbit forces which proves to be more severe than that afforded by mere examination of the magnetic moment of the deuteron.⁴

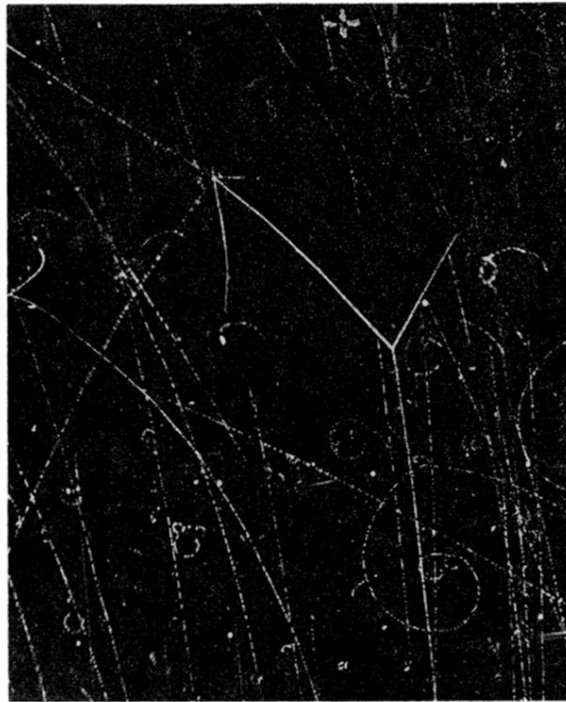


FIG. 1. $p\bar{p}$ scattering. The antiproton (denser track) enters from the top to the left of center. At an energy of 117 Mev, the antiproton scatters 41° to its left from a proton. The recoil proton has a range of 4.4 cm (49 Mev). The scattered antiproton comes to rest in 8.3 cm (68 Mev) and annihilates on a carbon nucleus, showing 5 visible prongs.



FIG. 3. An antiproton charge exchange. The antiproton is incident from the top and to the left of center, and the antiproton ending is indicated by an arrow. The antineutron from the charge-exchange process annihilates in the lower center of the picture. Five pions are produced in the annihilation with an energy release >1500 Mev.